

Analysis of positioning capabilities of 3GPP LTE

José A. del Peral-Rosado⁽¹⁾, José A. López-Salcedo⁽¹⁾, Gonzalo Seco-Granados⁽¹⁾,
Francesca Zanier⁽²⁾, and Massimo Crisci⁽²⁾

(1) *Universitat Autònoma de Barcelona (UAB), Spain*

(2) *European Space Agency (ESA), The Netherlands*

e-mails: JoseAntonio.DelPeral@uab.cat, Jose.Salcedo@uab.cat, Gonzalo.Seco@uab.cat,
Francesca.Zanier@esa.int, Massimo.Crisci@esa.int

BIOGRAPHY

José A. del Peral-Rosado received the M.Sc. in Electrical Engineering in 2009 and the Master Degree in Design of Telecommunication Systems in 2010 both from Universitat Autònoma de Barcelona (UAB). Currently, he is a PhD student at the Department of Telecommunications and Systems Engineering, Universitat Autònoma de Barcelona (UAB), and member of the Signal Processing for Communications and Navigation (SPCOMNAV) group.

Dr. **José A. López-Salcedo** received the M.Sc. and Ph.D. degrees in Telecommunication Engineering in 2001 and 2007, respectively, from Universitat Politècnica de Catalunya (UPC). From 2002 to 2006, he was a Research Assistant at UPC involved in R+D projects related with synchronization techniques for digital receivers, satellite communications and iterative decoding techniques for MIMO wireless systems, both for private industry and public administrations. Since 2006, he is Assistant Professor at the Department of Telecommunications and Systems Engineering, Universitat Autònoma de Barcelona (UAB), and member of the SPCOMNAV group.

Dr. **Gonzalo Seco-Granados** (SM'08) received the M.Sc. and Ph.D. degrees in Telecommunication Engineering in 1996 and 2000, respectively, from Universitat Politècnica de Catalunya (UPC). He also received an MBA from IESE-University of Navarra, Barcelona, in 2002. From 2002 to 2005, he was member of the technical staff at the European Space Research and Technology Center (ESTEC), European Space Agency (ESA), Noordwijk, The Netherlands, involved in the Galileo project and leading the activities concerning indoor GNSS. Since 2006, he is Associate Professor at the Department of Telecommunications and Systems Engineering, Universitat Autònoma de Barcelona (UAB), and member of the SPCOMNAV group. He was a co-guest editor for a special issue of the IEEE Signal Processing Magazine. Since 2009, he is Director of the Chair of Knowledge and Technology Transfer "UAB Research Park-Santander".

Dr. **Francesca Zanier** received the M.E. (cum laude) in Telecommunications Engineering and the PhD degree in Information Engineering from the University of Pisa (Italy). Since 2009, she has been with the Radionavigation section at ESA/ESTEC, Noordwijk, The Netherlands, working mainly on GNSS signal processing.

Dr. **Massimo Crisci** is the Head of Radio Navigation Systems and Techniques Section at the ESA. He is the technical domain responsible for the field of Radio Navigation. This encompasses, satellite RadioNav systems for satellite, aeronautical, maritime and land mobile users (including indoor) applications, future RadioNav equipment/techniques/receivers for (hybrid satellite/terrestrial) navigation/localisation systems for ground and space applications, signal in space design and end-to-end performance analysis for current/future radio navigation systems. He is the head of a team of Engineers providing RadioNav expert support to the various ESA programs (EGNOS and Galileo included). He holds a PhD in Automatics and Operations Research from the University of Bologna and a Master Degree in Electronics Engineering from University of Ferrara.

ABSTRACT

The performance of Global Navigation Satellite Systems (GNSS) can be improved in certain environments (e.g. indoor or urban scenarios) by using additional complementary systems, such as the use of wireless communications signals. Indeed, multicarrier wireless systems provide many advantages for the integration of both communications and positioning capabilities, such as the Long Term Evolution (LTE) that includes specific signals for positioning, i.e. the positioning reference signal (PRS). The assessment of the LTE positioning signals is not straightforward in realistic scenarios. Thus, a methodology is proposed for the theoretical analysis of the typical LTE position errors, by considering the joint impact of interferences and multipath. Preliminary results in an LTE coordinated network are shown using pedestrian and urban channel models.

1 INTRODUCTION

Most localization applications are nowadays based on Global Navigation Satellite Systems (GNSS). However, the robustness of mass-market GNSS receivers is compromised in challenging environments, such as indoor or urban scenarios. In these circumstances, the presence of blocking obstacles and propagation disturbances prevent them from observing the expected perfect clear-sky conditions that were assumed in the nominal design of the system. Complementary systems are usually proposed to assist the operation of GNSS systems.

Traditionally, cellular networks have provided the necessary assistance data to improve the overall performance, i.e. assisted-GNSS (A-GNSS), or estimated roughly the user position based on the cell radius, i.e. Cell-ID method. But recently, new positioning capabilities have been incorporated in order to satisfy two main drivers: legal mandates for location identification of emergency calls (e.g. E911 in US or E112 in Europe), and commercial applications or location-based services (LBS), such as navigation, advertising or social media. In this sense, the Long Term Evolution (LTE) technology, specified by the 3rd Generation Partnership Project (3GPP) consortium [1], has defined a dedicated downlink signal for Observed Time Difference of Arrival (OTDoA) positioning, i.e. the positioning reference signal (PRS). In fact, the LTE downlink is defined by a multicarrier Orthogonal Frequency Division Multiplexing (OFDM) signal, which is a well-known signal in wireless communications because of its flexibility, spectral efficiency and robustness against frequency-selective fading introduced by multipath, among other advantages with respect to traditional single-carrier signals.

The analysis of the positioning capabilities of LTE using OTDoA technique is of main interest in order to assess its potential as a complementary system to GNSS. In the literature, Medbo et al. obtained in [2] a positioning accuracy better than 20 m for 50% and 63 m for 95% of the cases using the measurements of a channel campaign. More recently, Gentner et al. studied in [3] the position error with a particle filter for a specific indoor scenario. A method to analyse the interference effect on the LTE position error was detailed in [4], but the presence of multipath was not considered. In addition, the 3GPP consortium has delivered several LTE positioning studies, such as in [5], but without publicising the procedure implemented. Therefore, this paper tries to find a methodology to theoretically analyse the typical position accuracy of LTE for different user locations, interference scenarios, multipath channels and PRS signal bandwidths. In Sec. 2, a description of the LTE standard is presented. The impact of inter-cell interferences and their effect on the OTDoA accuracy is described in Sec. 3 and 4, respectively. The impact of multipath on the time delay estimation is discussed in Sec. 5. Typical position errors are shown in Sec. 6, considering both interference and multipath. Finally, we draw the conclusions in Sec. 7.

2 LONG TERM EVOLUTION (LTE)

Long Term Evolution (LTE) moves towards the fourth generation (4G) of mobile communications. Most of its standard, which is driven by 3GPP, has been inherited from the Universal Mobile Telecommunication System (UMTS) in order to maintain backward compatibility. The main new features introduced are the downlink Orthogonal Frequency-Division Multiple Access (OFDMA) and the Multiple Input Multiple Output (MIMO) data transmission. The signal bandwidth is scalable from 1.4 MHz to 20 MHz with a symbol period T_s of 66.67 μ s, which corresponds to a subcarrier spacing F_{sc} of 15 kHz.

According to the LTE specification [6], the downlink positioning procedure, defined by the OTDoA method, uses the difference in the arrival times of downlink radio signals from multiple base stations (i.e. eNodeBs) to compute the user position. The method relies on a network-based strategy because the eNodeB locations are not provided to the user. First, the user equipment (UE) request assistance information to proceed with the timing measurements. Then, the LTE Positioning Protocol (LLP) transfers the UE measurements to the location server, E-SMLC (Enhanced Serving Mobile Location Center). Based on the UE measurements, the E-SMLC estimates the UE position using a trilateration technique, and this position information is finally sent back to the user.

Regarding to the physical layer, the LTE standard [7] specifies a set of downlink signals based on an OFDM modulation with different time-frequency distributions, whose basic structure is shown in Fig. 1 and 2. Downlink synchronization and reference signals are completely known (like the pilot signals in GNSS), and thus they are suitable for ranging purposes. Especially, the primary and secondary synchronization signal (i.e. PSS and SSS), as well as the cell-specific reference signal (CRS), can be used for signals of opportunity (SoO) applications because they do not require any assistance data. However, LTE follows the typical frequency reuse factor of a cellular network, which is equal to one. Thus, the received serving cell signal interferes with the received neighbour cell signals producing inter-cell interference, and resulting in the *near-far effect*. In order to obtain proper ranging measurements of the neighbour cells, the LTE standard in Release 9 specifies a **positioning reference signal** (PRS) that is especially dedicated for positioning purposes and mitigates the near-far effect, due to a higher frequency reuse factor (i.e. of six), by shifting one subcarrier position the frequency pilot allocation transmitted by each base station. The main parameters for PRS configuration are shown in Table 1. The PRS signal is scattered in time and frequency in the so-called *positioning occasion*, which allocates consecutive positioning subframes with a certain periodicity. The sophistication of this signal is even higher when the network mutes the PRS transmissions of certain base stations (i.e. PRS muting), in order to further reduce the inter-cell interference.

3 IMPACT OF INTER-CELL INTERFERENCES

The LTE localization performance can be deeply deteriorated due to the inter-cell interference among base stations. In this section, we identify three main interference scenarios while using the PRS signal (as proposed in [4]). The base stations are assumed to be fully synchronised and no clock offsets are considered.

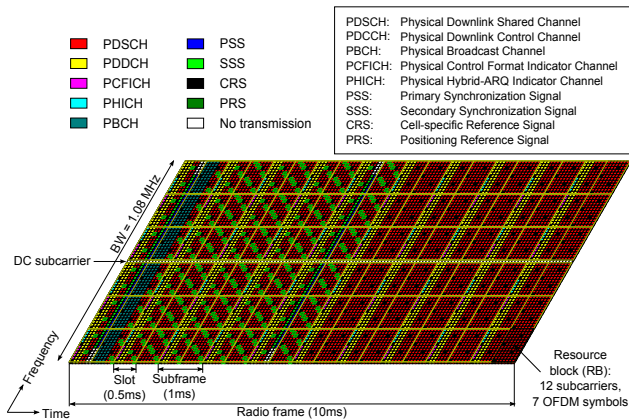


Fig. 1 Time-frequency grid of the LTE signals for 1.4 MHz bandwidth, FDD structure and normal cyclic prefix (CP).

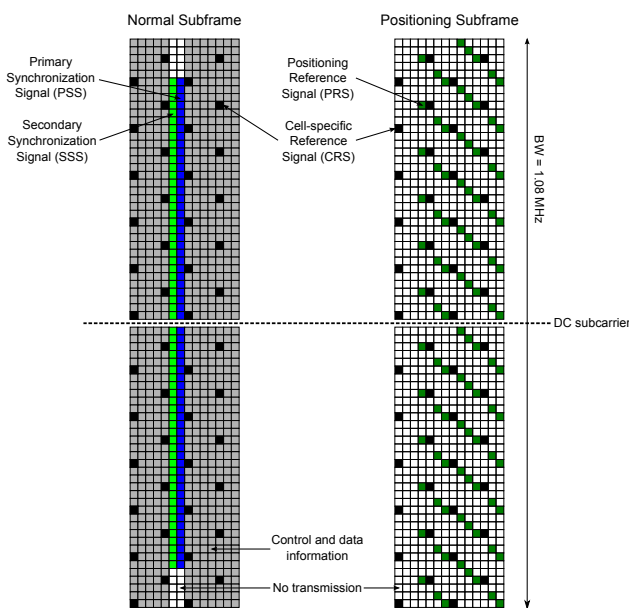


Fig. 2 Example of normal and positioning subframes with 6 resource blocks (RB) for one base station, FDD structure and normal cyclic prefix (CP).

Table 1 Main parameters of the PRS signal.

PRS bandwidth	1.4, 3, 5, 10, 15 and 20 MHz
PRS periodicity	160, 320, 640 or 1280 ms
Consecutive subframes	1, 2, 4, or 6
PRS muting information ¹	2, 4, 8, 16 bits
PRS pattern	6-reuse in frequency
PRS sequence	Length-31 Gold sequence

¹ Number of positioning occasion configured for PRS muting (i.e. bit equal to 0 when PRS is muted).

3.1 Non-coordinated network

The inter-cell interference is produced due to the single frequency transmission of the different base stations, as is typically planned in cellular networks for spectral efficiency. The received signal from neighbour cells is heavily masked by the strong signal of the serving cell, leading to the so-called near-far effect. Since the network provider decides if data is transmitted during positioning occasions, the PRS pattern can be used inefficiently by interfering the PRS pilots with data of neighbour cells, resulting on a non-coordinated network from the positioning point of view. Our analysis is based on the PRS signal over six resource blocks (RB), i.e. 12 pilot subcarriers along 1.08 MHz, and using only one OFDM symbol without cyclic prefix (CP). This interference LTE scenario is studied by means of a simulator implemented in MATLAB. The simulation follows the LTE standard [8], and creates a typical cell layout based on a hexagonal grid with three-sectorial base stations (i.e. 3 dB-beamwidth of 65-degree) and inter-site distance of 750 meters. Thus, considering the parameters summarized in Table 2, the received signal power from BS i is computed using the expression given in [8, p.14],

$$P_{rx,i} = P_{tx,i} - \max(L_i - G_{tx,i} - G_{rx}, \text{MCL}), \quad (1)$$

where $P_{tx,i}$ is the transmitted signal power, L_i is the macroscopic pathloss, $G_{tx,i}$ is the transmitter antenna gain, G_{rx} is the receiver antenna gain and MCL is the minimum coupling loss [8], defined as the minimum path loss between mobile and base station antenna connectors. This power budget is used to compute the signal-to-interference plus noise ratio (SINR) in an AWGN channel. The SINR is here defined as the ratio of signal power to the combined interference and noise power,

$$\text{SINR} = \frac{P_{rx,i}}{\sum_{j \neq i} P_{rx,j} + N_{rx}}, \quad (2)$$

where $P_{rx,j}$ is the received power from other antenna sectors, which causes the interference, and N_{rx} is the receiver noise floor. As it is shown in Fig. 3(a) for BS 1 and in Fig. 3(b) for BS 2, the SINR drastically decreases near the neighbour base stations, which shows the near-far effect produced by the serving base station.

3.2 Interference cancellation

In order to reduce the interference impact, the LTE research community is investigating on inter-cell interference coordination techniques to increase data transmission performance at critical positions of the cell layout, such as at the cell edge. An overview of these techniques can be found in [9], where the interference cancellation (IC) technique can be highlighted for 4G in general. The IC technique is based on reconstructing the signal from the strongest BS and subtracting it from the received signal, in order to obtain a superposition of the signals from the weaker base stations. Thus, we approximate the resulting SINR as

$$\text{SINR} = \frac{P_{rx,i}}{\sum_{\substack{j \neq i \\ j \neq m}} P_{rx,j} + N_{rx}}, \quad (3)$$

where $P_{rx,m}$ is the received power from the strongest BS. Supposing the IC technique is ideal (e.g. over the PRS signal), the SINR obtained for BS 1 and BS 2 is shown in Fig. 3(c) and Fig. 3(d). The IC technique is also investigated for positioning purposes by Mensing et al. in [10], and their results show an enhancement of the accuracy performance. Nevertheless, errors on the demodulation of the strongest BS signal may deteriorate the cancellation or even increase the interference. This is avoided when the interference source is a pilot signal (i.e. PSS, SSS or CRS signals).

3.3 Coordinated network

In general, a coordinated network is defined by the avoidance of data transmission from multiple base stations in the same frequency/slot, thus definitely reducing the interferences. The PRS characteristics are flexible enough in the LTE standard to create a coordinated network, by assuming no transmission of data on the PRS subframe. Although this coordinated scheme comes at the expense of decreasing the spectral efficiency, the interference avoidance is such that the SINR may be considered equal to the signal-to-noise ratio (SNR), as is shown in Fig. 3(e) and Fig. 3(f).

4 IMPACT OF INTERFERENCES ON THE OTDOA ACCURACY

Assuming the interferences to be Gaussian, the estimation of the user position, $\mathbf{x} = (x, y)^T$, can be assessed by means of the Cramér-Rao bound (CRB) for OTDOA localization. For this purpose, the K most powerful base stations with respect to position \mathbf{x} are considered, defining their locations by $\mathbf{x}_i = (x_i, y_i)^T$, where $i = 1, \dots, K$. The range between these base stations and the user is computed with the Euclidean distance of their positions as

$$d_i = |\mathbf{x} - \mathbf{x}_i| = \sqrt{(x - x_i)^2 + (y - y_i)^2}. \quad (4)$$

Table 2 Simulation parameters according to [8].

Parameter	Characteristic/value
<i>System</i>	
Carrier frequency	2 GHz
Bandwidth	1.4, 3, 5, 10, 15 and 20 MHz
Cell layout	Hexagonal
Inter-site distance	750 m
<i>Transmitter</i>	
Maximum BS power	43 and 46 dBm
BS antenna model	3 dB-beamwidth of 65-degree
BS antenna gain	15 dBi
<i>Receiver</i>	
UE antenna model	Omnidirectional, 0 dBi
UE noise figure	9 dB
Thermal noise density	-174 dBm/Hz
<i>Channel</i>	
Path loss model ¹	$128.1 + 37.6 \log_{10}(R)$ dB

¹ R is the propagation distance.

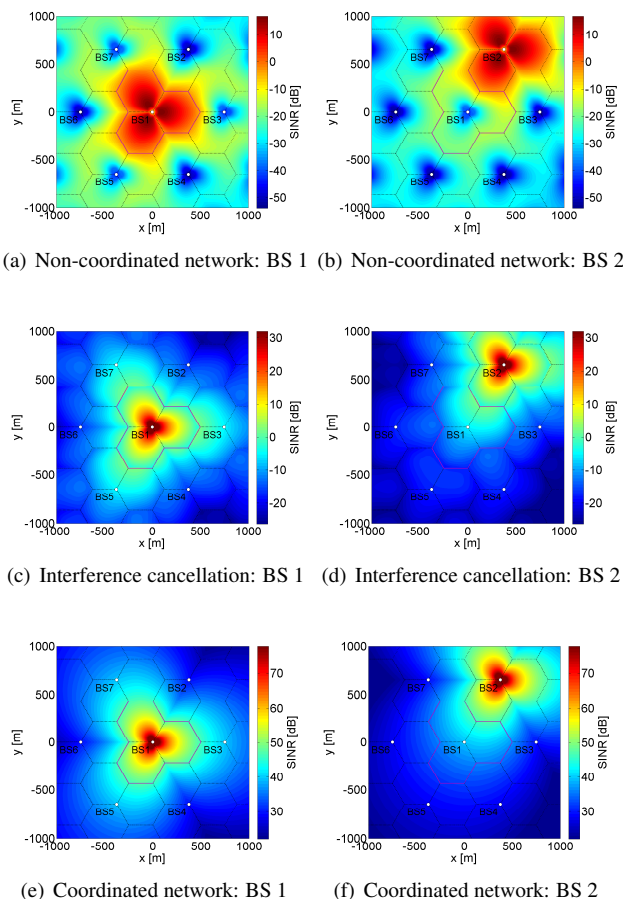


Fig. 3 SINR of BS 1 and BS 2 computed for the three general cases transmitting 6 RB of PRS signal.

The OTDoA localization is based on computing the difference of these range measurements. For this computation, the most powerful base station, whose location is \mathbf{x}_1 , is considered the reference BS. Thus, assuming no clock offsets, the LTE network can estimate range differences as

$$\hat{\mathbf{d}} = \mathbf{d} + \mathbf{n}, \quad \mathbf{n} \sim \mathcal{N}(0, \mathbf{R}), \quad (5)$$

where \mathbf{d} is defined as the true range differences vector,

$$\mathbf{d} = |\mathbf{x} - \mathbf{x}_1| - |\mathbf{x} - \mathbf{x}_j|, \quad j = 2, \dots, K, \quad (6)$$

and \mathbf{n} is a noise vector assumed to be additive white Gaussian noise (AWGN) with constant covariance matrix \mathbf{R} ,

$$\mathbf{R} = \begin{pmatrix} \sigma_1^2 + \sigma_2^2 & \sigma_1^2 & \cdots & \sigma_1^2 \\ \sigma_1^2 & \sigma_1^2 + \sigma_3^2 & \cdots & \sigma_1^2 \\ \vdots & \vdots & \ddots & \vdots \\ \sigma_1^2 & \sigma_1^2 & \cdots & \sigma_1^2 + \sigma_K^2 \end{pmatrix}, \quad (7)$$

being σ_i the standard deviation, which is defined by the root-mean-square error (RMSE) of the time delay for the signal transmitted from BS i . The general derivation of the CRB in AWGN channel can be found in [11, p.47], and it is applied for TDoA in [12, 13]. Although incurring in a penalty, as noted in [13] and [14], the covariance \mathbf{R} is approximated to be constant or non-dependant of the user position, thus the CRB for OTDoA localization results in

$$\text{CRB}(\mathbf{x}) = (\mathbf{D}^T \mathbf{R}^{-1} \mathbf{D})^{-1}, \quad (8)$$

where

$$\mathbf{D} = \begin{pmatrix} \frac{x-x_1}{d_1} - \frac{x-x_2}{d_2} & \frac{y-y_1}{d_1} - \frac{y-y_2}{d_2} \\ \frac{x-x_1}{d_1} - \frac{x-x_3}{d_3} & \frac{y-y_1}{d_1} - \frac{y-y_3}{d_3} \\ \vdots & \vdots \\ \frac{x-x_1}{d_1} - \frac{x-x_K}{d_K} & \frac{y-y_1}{d_1} - \frac{y-y_K}{d_K} \end{pmatrix}. \quad (9)$$

The position error in meters with respect to the true position \mathbf{x} is finally computed as

$$\varepsilon_{\mathbf{x}} = \sqrt{\text{tr}(\text{CRB}(\mathbf{x}))}. \quad (10)$$

5 IMPACT OF MULTIPATH ON TIME DELAY ESTIMATION

Propagation channel models are essential tools for simulation and testing of wireless transmission systems. The literature is extensive on this topic, and many standards have recommended channel models for specific propagation environments. These models may characterize path-loss attenuation, shadowing and multipath effects. Our interest is focused on the multipath propagation conditions present in typical LTE channels, and their impact on the time delay estimation of the PRS signal.

5.1 Tapped-delay line (TDL) channel models

The LTE standard adopts models based on the ITU-R M.1225 [15] recommendation and the 3GPP TS 05.05 [16] specification for GSM, widely used in the context of third generation mobile systems. The ITU and 3GPP models are defined by tapped-delay line (TDL) models, where each tap corresponds to a multipath signal characterized by a fixed delay, relative average power and Doppler spectrum. Their channel impulse response (CIR) is defined as

$$h(\tau; t) = \sum_{k=1}^K a_k \delta(\tau - \tau_k), \quad (11)$$

where K is the number of taps, τ_k is the tap delay relative to the first tap, and a_k is the Rayleigh-distributed complex amplitude of the tap, which follows a classical Jakes Doppler spectrum $S(f)$,

$$S(f) \propto \sqrt{\frac{1}{1 - (f/f_D)^2}}, \quad \text{for } f \in [-f_D, f_D], \quad (12)$$

being f_D the maximum Doppler shift.

Particularly, the 3GPP consortium agreed, in [17], on the use of the Pedestrian A and Vehicular A channels from [15], and the Typical Urban (TU) channel from [16], in order to model three reference environments characterized by a low, medium and large delay spread, respectively. Nevertheless, they were designed for a 5 MHz operating bandwidth, and an apparent periodicity appears in their frequency correlation properties for higher bandwidths [18]. Thus, the LTE standard has adopted since 2007 an extension of the ITU and 3GPP models by following the procedure described in [18], resulting in the Extended Pedestrian A (EPA), Extended Vehicular A (EVA) and Extended Typical Urban (ETU) channel models. The main parameters of these models, i.e. tap delay τ and signal-to-multipath ratio (SMR), are specified in Annex B of TS 36.101 [19] and TS 36.104 [20], and shown in Table 3. These specifications also define maximum Doppler shifts for each model to represent low, medium and high mobile conditions. Finally, the TDL models can be applied to multiple antenna schemes by introducing spatial correlation matrices, as it is discussed in [21], resulting on a simple LTE MIMO channel model.

5.2 Time delay estimation

Let us define the OFDM baseband signal format for one symbol used in the LTE downlink (without CP) as

$$x[n] = \sqrt{\frac{2 \cdot C}{N_c}} \sum_{k \in \mathcal{N}_a} p_k \cdot d_k \cdot \exp\left(j \frac{2\pi n k}{N_c}\right), \quad (13)$$

where C is the power of the band-pass signal, N_c is the number of subcarriers (excluding unused DC subcarrier),

Table 3 Tapped-delay line channel models parameters.

Tap no.	EPA channel		EVA channel		ETU channel	
	τ (ns)	SMR (dB)	τ (ns)	SMR (dB)	τ (ns)	SMR (dB)
1	0	0.0	0	0.0	0	-1.0
2	30	-1.0	30	-1.5	50	-1.0
3	70	-2.0	150	-1.4	120	-1.0
4	90	-3.0	310	-3.6	200	0.0
5	110	-8.0	370	-0.6	230	0.0
6	190	-17.2	710	-9.1	500	0.0
7	410	-20.8	1090	-7.0	1600	-3.0
8			1730	-12.0	2300	-5.0
9			2510	-16.9	5000	-7.0

\mathcal{N}_a is the subset of active pilot subcarriers N_a , which must satisfy $N_a \leq N_c$, d_k are the symbols, and p_k^2 is the relative power weight of subcarrier k , which is constrained by $\sum_k p_k^2 = N_c$ to give the nominal signal power C . In the presence of additive white Gaussian noise (AWGN), the received signal $r[n]$ is defined as

$$r[n] = x[n; n_\tau] + w[n], \quad (14)$$

where the discrete time delay (in samples) is $n_\tau = \tau \cdot F_s$, being F_s the sampling frequency, and $w[n]$ the noise component. Thus, the maximum likelihood estimation (MLE) for the AWGN channel is based on the correlation of the received signal $r[n]$ with a shifted and conjugated version of the reference signal $x[n]$, which is assumed periodical (i.e. circular correlation), in order to find the correlation peak. The resulting correlation between the received and the transmitted signal is defined by

$$R_{rx}(\tau) \doteq \sum_{n=0}^{N_c-1} r[n] \cdot x_c^*[n + n_\tau], \quad (15)$$

where $x_c[n]$ is a circular shifted version of the original $x[n]$, resulting in the matched filter of the OFDM signal, whose estimated delay is expressed as

$$\hat{\tau} = \frac{T_s}{N_c} \arg \max_{\tau} \left\{ |R_{rx}(\tau)|^2 \right\}, \quad (16)$$

where τ is the time delay in seconds. Thus, the maximum likelihood estimate for the AWGN channel is obtained by measuring the time delay corresponding to the maximum of the correlation function. In Fig. 4, the autocorrelation function of $x_c[n]$ is shown for different bandwidth configurations of the LTE positioning reference signal (PRS) using only one OFDM symbol. As it can be noticed, the bandwidth is denoted according to the number of resource blocks (RB) occupied by the PRS signal in the frequency domain (i.e. 180 kHz per RB).

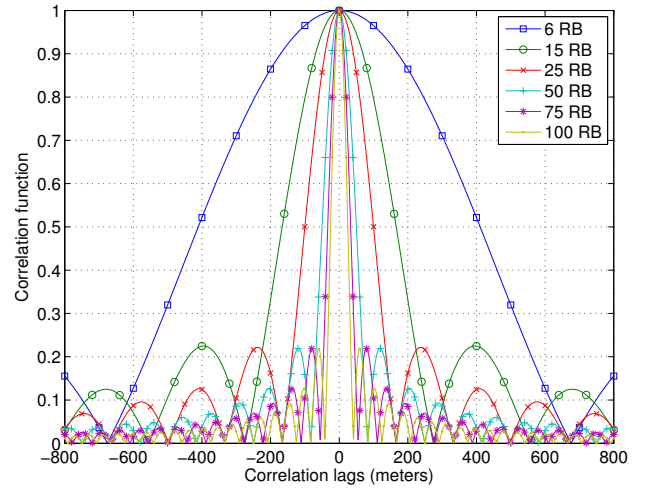


Fig. 4 Autocorrelation function of the LTE PRS signal for the different standard bandwidth and one OFDM symbol.

5.3 Timing error histogram in the acquisition process

The impact of the multipath channel can be assessed by computing the probability density function (PDF) of the time delay error. For that purpose, a large number of channel realisations is necessary to cover the majority of possible timing errors produced by multipath, from the statistical point of view. The timing errors are obtained by using the MLE for AWGN channel, that is, the time delay is estimated by finding the maximum peak of the convolution between the autocorrelation function of the LTE signal and the channel impulse response for each channel realisation. The histogram of the resulting timing errors finally shows the impact of the channel on the positioning in an acquisition-like process. This analysis is also of interest because it allows the assessment of the actual effect of multipath when nothing is done to compensate it. Particularly, since the multipath delays of the channel models specified in LTE (i.e. EPA, EVA and ETU channel models) are constant over time, we measure the impact produced by the complex amplitude variation of every multipath ray.

The Communications System ToolboxTM provided in MATLAB is used to perform the simulations. This toolbox contains the `stdchan` function to simulate multipath fading channels, where the LTE channel parameters of Table 3 can be introduced. In order to cover the maximum number of multipath ray combinations, a fast fading scenario is selected by defining a maximum Doppler shift of 300 Hz. The resulting histograms are shown in Fig. 5 for 20000 channel realisations and using a Savitzky-Golay FIR smoothing filter. The power delay profile (PDP) of the EPA, EVA and ETU channels is also added in order to identify which ray or group of rays may have caused a certain timing error.

As it could be expected, the PDP distribution characterizes the impact of the channel on the timing error. For instance,

the histograms for EPA channel, in Fig. 5(a), are centred on the multipath rays that concentrate more energy. Thus, many authors, such as [22] and [23], have used the mean delay, or the so-called *center of gravity*, of the PDP to provide an approximation of the delay error by computing a weighted average of the taps delays using the taps squared amplitude, defined by

$$\bar{\tau} = \frac{\sum_{k=1}^K \tau_k |a_k|^2}{\sum_{k=1}^K |a_k|^2}. \quad (17)$$

The mean delays of EPA, EVA and ETU models for the span of interest are 13, 47 and 59 meters, respectively. Nevertheless, as it was discussed in [24], this metric has to be carefully used because it may not characterize the typical timing estimate obtained for the actual multipath channel. The main constraint is posed by the signal bandwidth, which is not considered in the metric but which determines the ultimate shape of the correlation function. As it is shown in Fig. 4, the main lobe of the correlation function is narrowed when increasing the bandwidth, and thus the separation between multipath rays has to be lower in order to jointly contribute to the timing error. This effect can be especially noticed for high bandwidths, where one can easily identify the multipath rays in the timing error distributions, as it shown in Fig. 5.

5.4 Timing error histogram in the tracking process

Our interest is based on the analysis of the typical timing errors achieved with the LTE PRS signal. For that purpose, we consider a receiver stage where the LTE signal has been successfully acquired and fine tracking is provided. Under these circumstances, the time delay estimation is based, such as in [25], on finding the first peak (above the noise level) of the autocorrelation function when the multipath is applied, as it is shown in Fig. 6(a). Thus, the impact of both noise and multipath is considered in this procedure, hereby called *first-peak estimation*.

Using the procedure described, we can compute the cumulative density function (CDF) of the timing errors for a certain SNR, channel model and signal bandwidth. The resulting CDFs of the timing errors for EPA and ETU channels models with a SNR equal to 25 dB are shown in Fig. 6(b) and 6(c), respectively. As it can be noticed, the ETU case has larger errors than the EPA case, especially for low signal bandwidths (e.g. 6 RB or 1.08 MHz). At low bandwidths, the current procedure is equal to the one presented in the previous section, because all the multipath rays jointly contribute on the timing error forming a single peak on the estimation function (i.e. convolution between the autocorrelation and the CIR). Thus, the mean delay of the PDP $\bar{\tau}$ is around the 50% of the cases of the CDF, as

noticed in Fig. 6(b) and 6(c). Since the mean delay is lower for EPA model than for ETU model, the mean pseudorange errors obtained are lower too. As it can be assessed, the impact of the multipath channel is limited by the models applied, mainly due to the fixed taps delays modelled.

In order to have a measure of the typical timing or pseudorange errors obtained with LTE in these scenarios, the 67% and 95% of the cases of the computed CDF are chosen. These values can also be compared with those stated within E911 and E112 requirements.

6 IMPACT OF BOTH INTERFERENCE AND MULTIPATH

The analysis of the LTE PRS signal has just been focused on the impact of noise and multipath, but interference is a major impairment in LTE that must be definitely taken into account. For that purpose, the tools previously described are combined to compute the typical position errors for an LTE coordinated network (i.e. from the interference point of view) in a pedestrian and urban scenario, characterized by EPA and ETU channel models, respectively.

If we assume that the signals transmitted from the five most powerful base stations with respect to the user position are received and used for OTDoA localisation, the link budget for every base station and user location can be computed following the procedure described in Sec. 3. Thus, five signal-to-interference plus noise ratio (SINR) values are obtained for every user location considering a certain bandwidth, and are used to determine the noise level for a certain link between base station and user. Once the AWGN noise is added to the signal, its autocorrelation is convolved with the channel impulse response of a specific multipath model. Then, the first-peak estimation technique is used to compute the cumulative density function (CDF) of the pseudorange errors. Finally, the 67% or 95% values of the CDF are taken for the specific SINR, channel model and signal bandwidth to obtain the final user position error with the CRB for OTDoA localisation.

Following the procedure described above, the resulting position errors are shown in a two-dimensional map at every user location in Fig. 7, and they can be compared with the results in the absence of multipath presented in [4]. As it can be noticed, the best position accuracy is around the barycentre of every three close base stations. For an EPA channel using a bandwidth of 6 RB (i.e. 1.08 MHz), the lowest position error is around 12 and 30 meters in the 67% and 95% of the cases, as is shown in Fig. 7(a) and 7(b), respectively. These position errors can be improved if the signal bandwidth is increased up to 100 RB (i.e. 18 MHz), resulting in position errors around 4 and 10 meters in the 67% and 95% of the cases for an EPA channel, as is shown in Fig. 7(c) and 7(d), respectively. Similar results can only be obtained for an ETU channel when using high bandwidths, as in Fig. 7(e) and 7(f), because of the higher mean

delay of the channel impulse response, as commented in the previous section. As it can be noticed, these results are highly dependent on the channel model and the estimation technique.

7 CONCLUSION

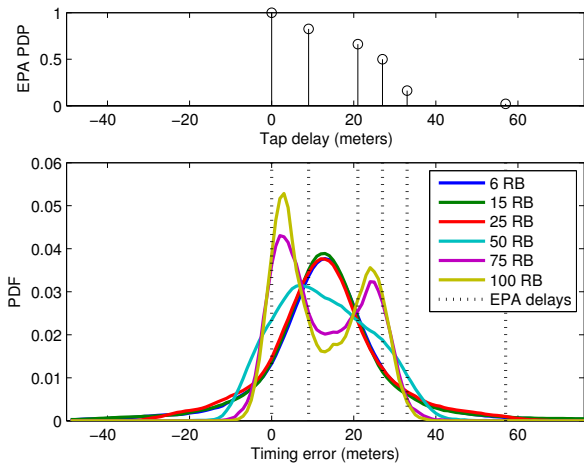
The positioning capabilities of the Long Term Evolution (LTE) positioning reference signal (PRS) have been analysed considering the impact of noise, inter-cell interference and multipath. For that purpose, the link budget of the five most powerful base stations with respect to the user location have been computed for every position in an LTE coordinated network. The resulting signal-to-interference plus noise ratio (SINR) values have been used to determine the AWGN noise level, which has been added to the PRS signal. The autocorrelation of the signal plus noise has been convolved with the channel impulse response of a typical multipath model (i.e. EPA or ETU model). Then, the *first-peak estimation* technique has been used to compute timing errors for every channel realisation. Typical pseudorange values have been computed with the 67% and 95% of the cumulative density function (CDF) of the timing errors obtained. These pseudoranges have been finally used to compute the position error by means of the CRB for OTDoA localization. Using the lowest bandwidth of LTE (i.e. 1.08 MHz), typical position errors around 12 and 30 meters have been found in the 67% and 95% of the cases for an EPA channel, respectively. These results improve for the highest signal bandwidth (i.e. 18 MHz) up to 4 and 10 meters in the 67% and 95% of the cases with the same channel, respectively. In the ETU channel, position errors around 10 meters have only been obtained for high bandwidth. Thus, a methodology for the theoretical analysis of typical LTE position errors has been proposed, and preliminary results have been shown for an LTE coordinated network.

ACKNOWLEDGMENT

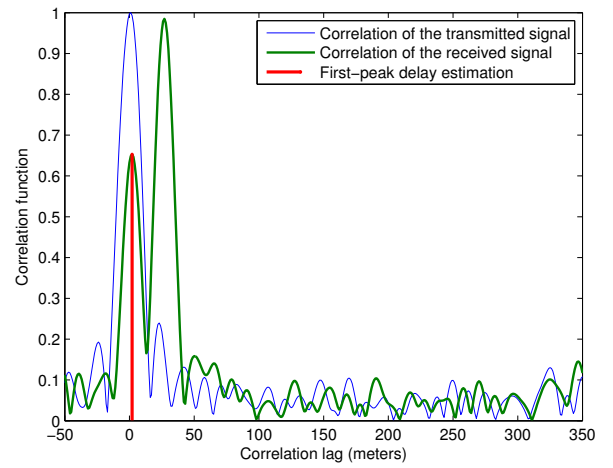
The content of the present article reflects solely the authors view and by no means represents the official European Space Agency (ESA) view. This work was supported by the ESA under the PRESTIGE programme ESA-P-2010-TEC-ETN-01 and by the Spanish Ministry of Science and Innovation project TEC 2011-28219.

REFERENCES

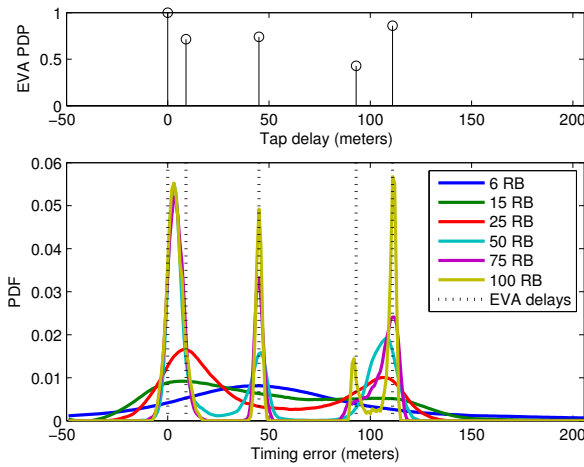
- [1] 3GPP home page. [Online]. Available: www.3gpp.org
- [2] J. Medbo, I. Siomina, A. Kangas, and J. Furuskog, "Propagation channel impact on LTE positioning accuracy: A study based on real measurements of observed time difference of arrival," in *Proc. IEEE PIMRC '09*, Sept. 2009, pp. 2213–2217.
- [3] C. Gentner, E. Muñoz, M. Khider, E. Staudinger, S. Sand, and A. Dammann, "Particle filter based positioning with 3GPP-LTE in indoor environments," in *Proc. IEEE/ION PLANS '12*, april 2012, pp. 301–308.
- [4] J. A. Del Peral-Rosado, J. A. López-Salcedo, G. Seco-Granados, F. Zanier, and M. Crisci, "Achievable Localization Performance Accuracy of the Positioning Reference Signal of 3GPP LTE," in *Proc. ICL-GNSS*, June 2012.
- [5] R1-091789, "Further considerations on PRS design for LTE Rel-9," 3GPP, Huawei, May 2009.
- [6] 3GPP TS 36.305, *Stage 2 functional specification of User Equipment (UE) positioning in E-UTRAN*, Std.
- [7] 3GPP TS 36.211, *Physical Channels and Modulation*, Std.
- [8] 3GPP TR 36.942, *RF system scenarios*, Std.
- [9] G. Boudreau, J. Panicker, N. Guo, R. Chang, N. Wang, and S. Vrzic, "Interference coordination and cancellation for 4G networks," *IEEE Communications Magazine*, vol. 47, no. 4, pp. 74–81, April 2009.
- [10] C. Mensing, S. Sand, A. Dammann, and W. Utschick, "Interference-aware location estimation in cellular OFDM communications systems," in *Proc. IEEE ICC*, June 2009.
- [11] S. Kay, *Fundamentals of Statistical Signal Processing: Estimation Theory*. Prentice-Hall PTR, 1993–1998.
- [12] Y. T. Chan and K. C. Ho, "A simple and efficient estimator for hyperbolic location," *IEEE Trans. on Signal Processing*, vol. 42, no. 8, pp. 1905–1915, Aug. 1994.
- [13] R. Kaune, J. Horst, and W. Koch, "Accuracy analysis for TDOA localization in sensor networks," in *Proc. IEEE FUSION*, July 2011.
- [14] Y. Wang, G. Leus, and A.-J. van der Veen, "Cramer-Rao bound for range estimation," in *Proc. IEEE ICASSP*, April 2009, pp. 3301–3304.
- [15] ITU-R M.1225, "Guidelines for evaluation of radio transmission technologies for IMT-2000," 1997.
- [16] 3GPP TS 05.05, *Radio transmission and reception*, Std.
- [17] R4-070572, "Proposal for LTE channel models," 3GPP, Ericsson, Nokia, Motorola, Rohde & Schwarz, RAN4-43, May 2007.
- [18] T. Sorensen, P. Mogensen, and F. Frederiksen, "Extension of the ITU channel models for wideband (OFDM) systems," in *Proc. IEEE VTC '05*, vol. 1, Sept. 2005, pp. 392–396.
- [19] 3GPP TS 36.101, *UE radio transmission and reception*, Std.
- [20] 3GPP TS 36.104, *BS radio transmission and reception*, Std.
- [21] R4-060334, "LTE Channel Models and simulations," 3GPP, Ericsson, Elektrobit, Nokia, Motorola, Siemens, RAN4-38, Feb. 2006.
- [22] R1-092307, "Analysis of UE subframe timing offset measurement sensitivity to OTDoA performance," 3GPP, Alcatel-Lucent, June 2009.
- [23] C. Mensing and A. Dammann, "Positioning with OFDM based communications systems and GNSS in critical scenarios," in *Proc. WPNC '08*, Mar. 2008, pp. 1–7.
- [24] J. A. Del Peral-Rosado, J. A. López-Salcedo, G. Seco-Granados, F. Zanier, and M. Crisci, "Evaluation of the LTE Positioning Capabilities Under Typical Multipath Channels," in *Proc. ASMS/SPSC '12*, Sept. 2012.
- [25] N. Chen, M. Tanaka, and R. Heaton, "OFDM timing synchronisation under multi-path channels," in *Proc. IEEE VTC '03-Spring*, vol. 1, April 2003, pp. 378–382.



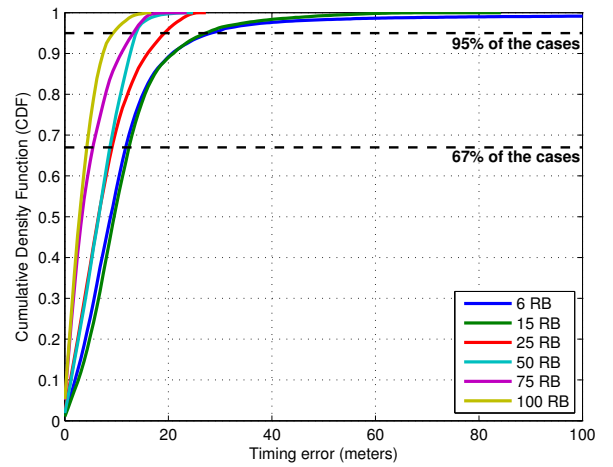
(a) EPA channel model



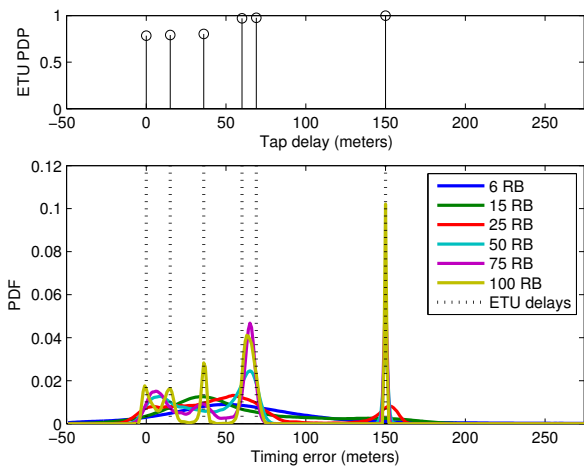
(a) EPA channel model, 100 RB



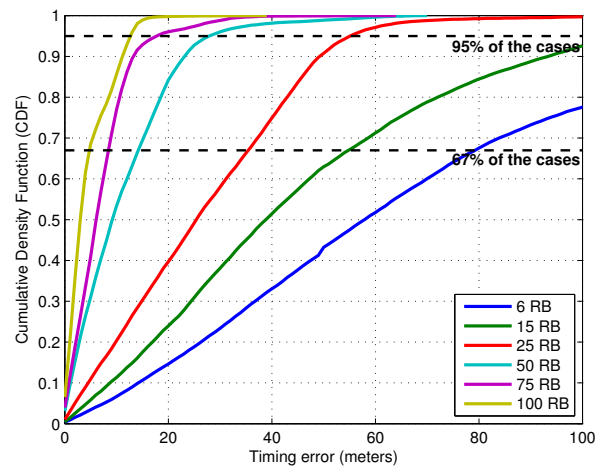
(b) EVA channel model



(b) CDF for EPA channel model



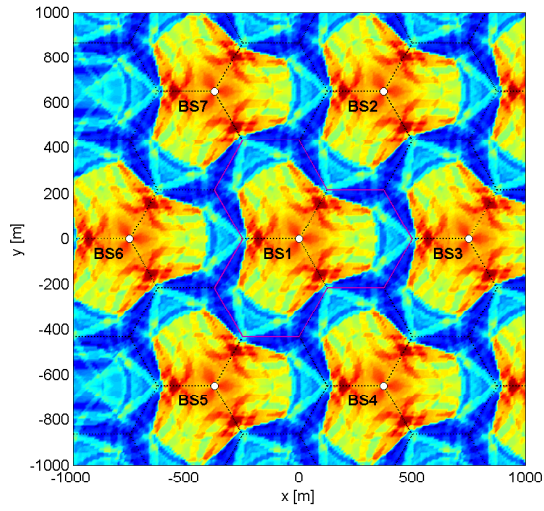
(c) ETU channel model



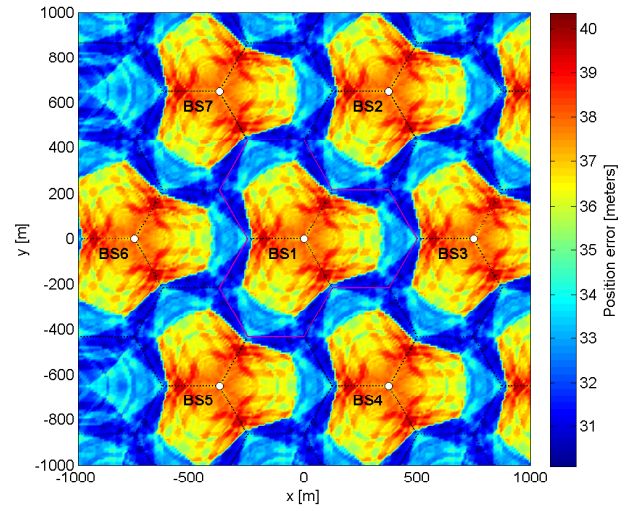
(c) CDF for ETU channel model

Fig. 5 Timing error histograms of the MLE for the AWGN channel using TDL channel models.

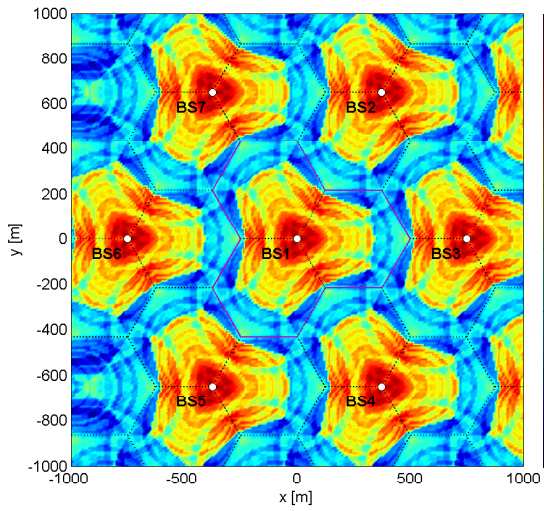
Fig. 6 Pseudorange results using first-peak estimation for a SNR equal to 25 dB.



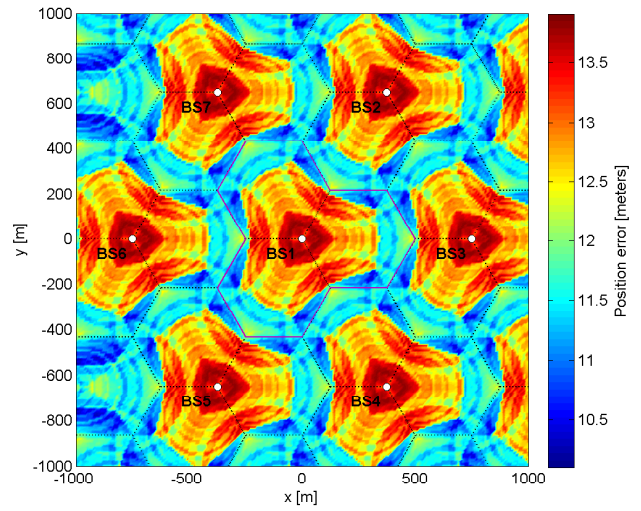
(a) 67% of the CDF of EPA channel, 6 RB



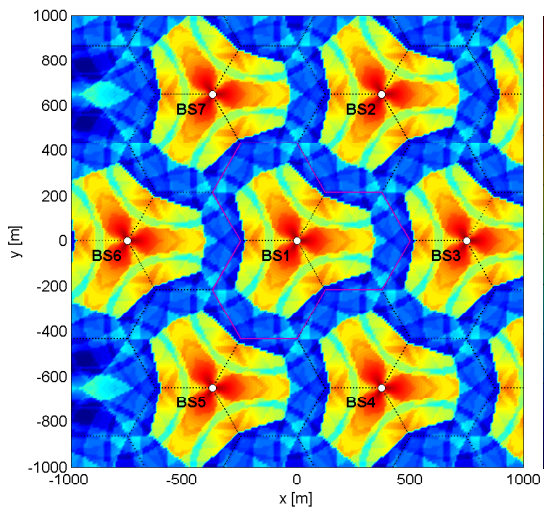
(b) 95% of the CDF of EPA channel, 6 RB



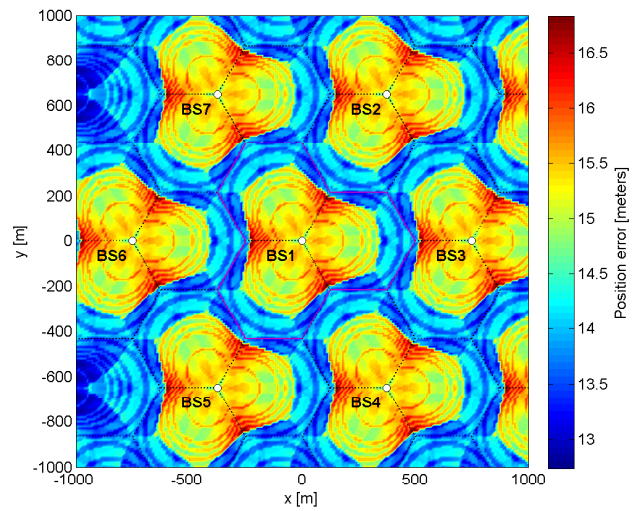
(c) 67% of the CDF of EPA channel, 100 RB



(d) 95% of the CDF of EPA channel, 100 RB



(e) 67% of the CDF of ETU channel, 100 RB



(f) 95% of the CDF of ETU channel, 100 RB

Fig. 7 Typical position errors for the PRS signal in an LTE coordinated network.